

Switched Control Design for Quadrotor in Target Tracking with Complex Intermittent Measurements

Liang, Ye; Yang, Jianan; Zhang, Lixian; Baldi, Simone; De Schutter, Bart

DOI

[10.2514/1.G006599](https://doi.org/10.2514/1.G006599)

Publication date

2023

Document Version

Final published version

Published in

Journal of Guidance, Control, and Dynamics

Citation (APA)

Liang, Y., Yang, J., Zhang, L., Baldi, S., & De Schutter, B. (2023). Switched Control Design for Quadrotor in Target Tracking with Complex Intermittent Measurements. *Journal of Guidance, Control, and Dynamics*, 46(1), 206-214. <https://doi.org/10.2514/1.G006599>

Important note

To cite this publication, please use the final published version (if applicable). Please check the document version above.

Copyright

Other than for strictly personal use, it is not permitted to download, forward or distribute the text or part of it, without the consent of the author(s) and/or copyright holder(s), unless the work is under an open content license such as Creative Commons.

Takedown policy

Please contact us and provide details if you believe this document breaches copyrights. We will remove access to the work immediately and investigate your claim.

Green Open Access added to TU Delft Institutional Repository

'You share, we take care!' - Taverne project

<https://www.openaccess.nl/en/you-share-we-take-care>

Otherwise as indicated in the copyright section: the publisher is the copyright holder of this work and the author uses the Dutch legislation to make this work public.



Engineering Notes

Switched Control Design for Quadrotor in Target Tracking with Complex Intermittent Measurements

Ye Liang,* Jianan Yang,† and Lixian Zhang‡
Harbin Institute of Technology, 150001 Harbin,
People's Republic of China

Simone Baldi§^{ORCID}
Southeast University, 210000 Nanjing,
People's Republic of China

and
Bart De Schutter¶
Delft University of Technology, 2628 CD Delft,
The Netherlands

<https://doi.org/10.2514/1.G006599>

Nomenclature

A_m, A_u	=	controller gains matrices of measurable subsystems and unmeasurable subsystems
\mathbb{U}^*	=	designed switched controller with energy-dependent gains
u_1, u_2, u_3, u_4	=	quadrotor controllers
x, y, z	=	position of the quadrotor, m
x_t, y_t	=	target position, m
θ, ϕ, ψ	=	attitude of the quadrotor, rad

I. Introduction

STUDIES on target tracking of quadrotors have spanned quite a few decades, motivated by their extensive applications in aerial imaging and mapping [1,2], searching and rescuing [3], autonomous landing [4,5], etc. The control objective in the target tracking task is to make the quadrotor maintain a given distance to the target, which can be achieved using different control methods developed in the past years, e.g., sliding mode control [6,7], robust control [8,9], and adaptive control [10,11]. In the existing studies, the distance of the quadrotor to the target is assumed to be continuously measured by on-board sensors such as cameras and radars. Clearly, it is too ideal to assume that measurements from sensors are always available since the complexity of scenes and the limitations of measuring algorithms, e.g., feature mismatching, target misrecognition, or obstacle blocking, prevent from having constant measurements. In these scenarios, the target may be undetected once in a while, which means that the

feedback for quadrotor tracking control is intermittently available and may cause task failure.

In the case of target loss, the feedback for the quadrotor control system is unavailable, so that the quadrotor will hover at the current position until the target can be measured again. Under such circumstances, the target may get out of the field of view (FOV) of the sensors and may never return into the FOV, which often causes the quadrotor to give up the tracking task. To tackle the problem of target tracking with intermittent measurements, some studies focus on the precise estimation of the target motion when losing the target by learning-based [12] or filter-based [13] methods, and other studies use path planning to drastically change the motion of the quadrotor to keep the target stay in the FOV [14]. However, the methods above require high-performance computing resources resulting in low applicability. The switched systems scheme is considered in quite a few studies [15–17] as a low computing alternative to tracking control: the switched systems approach allows to formulate the process of target tracking by splitting it into two subsystems, i.e., a *measurable subsystem*** and an *unmeasurable subsystem*,* according to whether the target can be measured or not. Then, the target tracking task can be regarded as a stabilization problem for such a switched system. Note that the unmeasurable subsystem will be affected by a disturbance that is caused by inevitable estimation errors since the target motion must be estimated, which may lead to an increase of the tracking system energy. When controllers are *predesigned* for ensuring the stability of each subsystem [15–17], the problem becomes the one of deriving certain running time conditions such that the increase of energy during the running time of the unmeasurable subsystem can be counteracted by the decrease during the running time of the measurable subsystem, which ultimately ensures the stability of the underlying system. However, such a method via the proposed predesigned controllers will apply only to the stability analysis since the running time conditions cannot always be satisfied in practice. Compared with the determination of running time conditions using predesigned controllers for subsystems, the controller design (in a stabilizing manner) for the whole switched system for actual running time (random and undesignable) of subsystems is more applicable and quite open. Also, how to determine the controller gains for the stages of the switching (with different system energy), allowing not only for system stability but also for performance benefits, is worthwhile further investigations.

It is worth noting that the aforementioned methods in [15–17] model the underlying system in the framework of dwell time switching, which requires that the running time of each activated measurable subsystem is not less than a constant dwell time. Unfortunately, such an assumption may not be qualified for most of the target tracking tasks of quadrotors if there does not only exist slow switching (the running time is greater than the dwell time) but also exist fast switching (otherwise). Fast switching is not seldom encountered in target tracking because the measurements may last very shortly when sensors are disturbed by random noise or the target is observed through the crack between obstacles. In such cases, it is difficult to find a minimum time interval as the dwell time in the system formulation. To improve the applicability for quadrotors in tracking tasks with above complex intermittent measurements, it is required to find a new switched systems scheme to overcome the limitation of the certain running time conditions. However, the formulated switched systems in existing literature cannot cover the possible fast switching, such that corresponding

Received 28 November 2021; revision received 30 June 2022; accepted for publication 4 October 2022; published online 8 November 2022. Copyright © 2022 by the American Institute of Aeronautics and Astronautics, Inc. All rights reserved. All requests for copying and permission to reprint should be submitted to CCC at www.copyright.com; employ the eISSN 1533-3884 to initiate your request. See also AIAA Rights and Permissions www.aiaa.org/randp.

*Ph.D. Candidate, School of Astronautics; liangye@hit.edu.cn.

†Ph.D. Candidate, School of Astronautics; jnyang@hit.edu.cn (Co-Corresponding Author).

‡Professor, School of Astronautics; lixianzhang@hit.edu.cn (Corresponding Author).

§Professor, School of Mathematics; s.baldi@tudelft.nl.

¶Professor, Delft Center for Systems and Control; b.deschutter@tudelft.nl.

**In this paper, we slightly abuse the notions of measurable subsystem and unmeasurable subsystem to mean that the target motion is measurable and unmeasurable, respectively.

stability conditions and control methods are not suitable in these scenarios, which motivates this study.

In this paper, we are interested in dealing with the problem of controller design for the quadrotor in target tracking with complex intermittent measurements, where the duration of measurements is not limited by a constant.

The main contributions of the work are twofold:

1) A new switched systems scheme is formulated to cover the case that the duration of measurements may be fairly short, in addition to the case in existing studies that the running time of the underlying system with measurements should be no less than a constant.

2) The switched controller with energy-dependent gains is designed for the issue of quadrotor position control, which determines the gains by considering the different system energy in various stages, and which ensures the rapid tracking capability of the quadrotor and guarantees the stability of the closed-loop target tracking system.

The remainder of this paper is organized as follows: Section II presents the considered problem and preliminaries. The control scheme and the formulated switched tracking system are introduced in Sec. III. In Sec. IV, the derived stability condition and the designed switched controller are given. Simulations are provided to verify the advantages of the switched control design in Sec. V, and Sec. VI concludes this paper.

II. Preliminaries and Problem Statement

In the target tracking tasks of the quadrotor, the goal is to design a controller to regulate the tracking error as small as possible. Figure 1 illustrates a general scenario of target tracking of a quadrotor, where the position and the velocity of the quadrotor are obtained by a Global Positioning System (GPS) and accelerometers, respectively, and the target (e.g., an unmanned ground vehicle) is located by an on-board sensor fixed by a gimbal. The body frame \mathcal{F}_b of the quadrotor is established, where the origin is fixed at the gravity center, and the x axis, y axis, and z axis are aligned with the motion of forward, left, and altitude, respectively. Then, the tracking frame \mathcal{F}_t is defined by the initial body frame, where the origin is fixed at the initial position of the quadrotor and the axes directions are the same as the initial directions of \mathcal{F}_b . The quadrotor tracks the target in the horizontal xy -plane with a fixed altitude and a constant heading angle at \mathcal{F}_t , and the direction of the FOV of the on-board sensor is regulated by the gimbal to keep toward the target.

The quadrotor control system is underactuated, where six-dimensional motion states are driven by four-dimensional controllers. As shown in Fig. 1, the states for quadrotor position control are denoted by x , y , and z along the axes, and the corresponding states for quadrotor attitude control are denoted by θ , ϕ , and ψ , respectively. The adopted mathematical model (cf. [17]) of the quadrotor in this paper can be given by

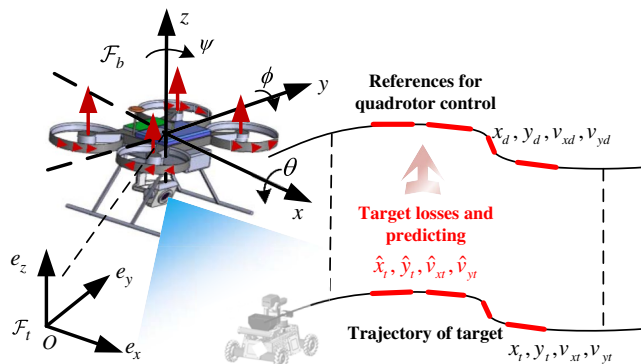


Fig. 1 Illustration of target tracking of a quadrotor with intermittent measurements.

$$\begin{cases} \ddot{x} = -u_1(\cos\phi\sin\theta\cos\psi + \sin\phi\sin\psi) \\ \ddot{y} = -u_1(\cos\phi\sin\theta\sin\psi - \sin\phi\cos\psi) \\ \ddot{z} = u_1(\cos\phi\cos\theta) - 1 \\ \ddot{\theta} = u_2 \\ \ddot{\phi} = u_3 \\ \ddot{\psi} = u_4 \end{cases} \quad (1)$$

where u_1 , u_2 , u_3 , and u_4 are the control inputs, and they are determined by current propeller lift forces, gravity, and other physical constants of the quadrotor (cf. [18] for more details). Since quadrotors commonly run under the small-angle variation (cf. [17,19]) in target tracking tasks, Eq. (1) can be converted to

$$\begin{cases} \ddot{x} = -u_1\theta \\ \ddot{y} = u_1\phi \\ \ddot{z} = u_1 - 1 \end{cases} \quad \begin{cases} \ddot{\theta} = u_2 \\ \ddot{\phi} = u_3 \\ \ddot{\psi} = u_4 \end{cases} \quad (2)$$

When the target distance can be measured by on-board sensors, the target position $(x_t, y_t, 0)$ is simply obtained by adding the measured distance to the quadrotor position located by GPS, then the target velocity $(v_{xt}, v_{yt}, 0)$ can be determined by derivation. According to the given constant distance requirements, the reference position (x_d, y_d, z_d) can be obtained using the target position $(x_t, y_t, 0)$, while the reference velocity (v_{xd}, v_{yd}) is equal to the velocity of the target (v_{xt}, v_{yt}) . When the target distance is unmeasurable, i.e., the target motion (position and velocity) cannot be obtained, a motion predictor is utilized to obtain the target motion $(\hat{x}_t, \hat{y}_t, \hat{v}_{xt}, \hat{v}_{yt})$ for providing an estimated reference signal. Thus, the tracking process can be formulated under a switched systems scheme [15–17] with inevitable disturbance, i.e., the prediction error. For the stability analysis of the switched systems, the time interval consisting of running time of consecutive subsystems can be regarded as a *stage* of switching. Then, the switched system is said to be globally uniformly ultimately bounded (GUUB) if the initial values of the Lyapunov function (plays the role of an energy-like function for the tracking system) between consecutive stages decrease, and the Lyapunov function decreases or increases under an upper bound within a stage (cf. [20]), when the value of the Lyapunov function is greater than the given ultimate bound. It is worth mentioning that the stability of the switched system is ensured by satisfying certain running time conditions in the existing literature [15–17], which may be not satisfied in practice, let alone in the case of complex intermittent measurements, e.g., the measurements of the quadrotor last fairly short. Besides, in the aforesaid studies, predesigned controllers are utilized, which are given to ensure the stability of each subsystem without consideration of the performance of the whole switched system, e.g., the convergence rate, and the steady-state tracking error attenuation.

The objectives of this paper are to formulate a new switched system scheme for modeling the target tracking process with complex intermittent measurements, and to design a superior controller for the underlying system to ensure that the quadrotor approaches the target rapidly and simultaneously keeps the tracking error as small as possible.

III. Quadrotor Tracking Control System

A hierarchical control framework is utilized for quadrotor control, which is composed of an inner attitude control loop and an outer position control loop. As shown in Fig. 2, the reference signals z_d and ψ_d are given constants such that the quadrotor moves with a fixed altitude and a constant heading angle, while the reference signals x_d , y_d , v_{xd} , and v_{yd} can be obtained by measuring the target motion (when it is measurable) or by predicting it (otherwise).

A. Attitude Control

This subsection is devoted to the design of the attitude controllers consisting of u_2 , u_3 , and u_4 . As the inner loop of the quadrotor control

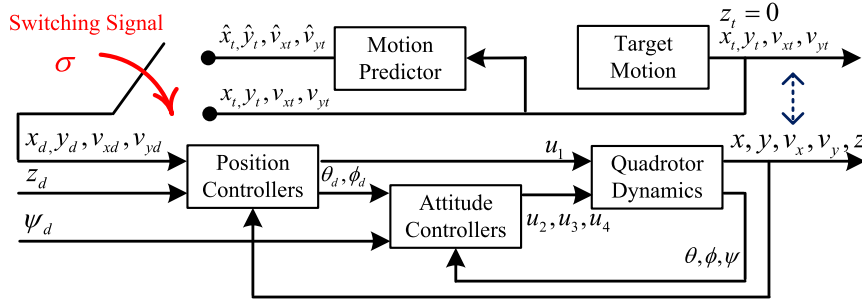


Fig. 2 Quadrotor control framework for target tracking with intermittent measurements.

system, a rapid response capability is necessary since it is significant for the overall system to achieve satisfactory performance. The non-singular terminal sliding mode control (NTSMC) [21] method is adopted in this paper since not only it has advantages of conventional sliding mode control (SMC) strategies, i.e., insensitivity to model errors, parametric uncertainties, and diverse disturbances, but also it can regulate the state to reach its reference in finite time by a terminal attractor. The sliding curves with terminal attractors utilized for adjusting all inner-loop states are the same, and they are designed by $s_i = c_i + \beta \dot{c}_i^{p/q}$, where $i \in \{\phi, \theta, \psi\}$ denotes the attitude dynamics, $c_i = i - i_d$ is the difference between the state and the reference, β is a positive number, and p and q are positive odd integers satisfying $1 < p/q < 2$ to avoid singularities. By computing the derivative of s_i , one has

$$\dot{s}_i = \dot{c}_i + \beta \frac{p}{q} \dot{c}_i^{(p/q)-1} \dot{c}_i = \dot{i} - \dot{i}_d + \beta \frac{p}{q} (\dot{i} - \dot{i}_d)^{(p/q)-1} (\ddot{i} - \ddot{i}_d) \quad (3)$$

It is worth mentioning that $\ddot{i}_d = 0$ at steady state. Then, considering the sliding mode condition $\dot{s}_i = 0$, and the system dynamics $u_k = \ddot{i}$ ($k \in \{2, 3, 4\}$), the attitude controller is designed as follows:

$$u_k = -\frac{1}{\beta} \frac{q}{p} (\dot{i} - \dot{i}_d)^{2-(p/q)} - K \text{sgn}(s_i) \quad (4)$$

where K is a positive real number. For the Lyapunov function candidate $V(s_i) = (1/2)s_i^2$, we have

$$\begin{aligned} \dot{V}(s_i) &= \frac{1}{2} \frac{d}{dt} s_i^2 = s_i \dot{s}_i \\ &= s_i \cdot \left(\dot{i} - \dot{i}_d + \beta \frac{p}{q} (\dot{i} - \dot{i}_d)^{(p/q)-1} \cdot \left(-\frac{1}{\beta} \frac{q}{p} (\dot{i} - \dot{i}_d)^{2-(p/q)} - K \text{sgn}(s_i) \right) \right) \\ &= -s_i \cdot \beta \frac{p}{q} (\dot{i} - \dot{i}_d)^{(p/q)-1} K \text{sgn}(s_i) \leq -K \beta \frac{p}{q} (\dot{i} - \dot{i}_d)^{(p/q)-1} |s_i| \end{aligned} \quad (5)$$

Since p and q are positive odd integers satisfying $1 < p/q < 2$, we have $(\dot{i} - \dot{i}_d)^{(p/q)-1} > 0$ in the case of $\dot{i} - \dot{i}_d \neq 0$, and then the Lyapunov stability is satisfied. When $\dot{i} - \dot{i}_d = 0$, one has $\ddot{i} - \ddot{i}_d = -K \text{sgn}(s_i)$, where $\ddot{i} - \ddot{i}_d = 0$ only if $s_i = 0$. Thus, the sliding curve can be reached for any value of states (cf. [21] for more details). Therefore, applying the designed controller (4), the values of the inner-loop states ϕ , θ , and ψ will converge to the references ϕ_d , θ_d , and ψ_d , respectively.

B. Position Control

Proportional–derivative (PD) controllers are utilized for the quadrotor outer-loop position control, where the states can be divided into a fully actuated state z and two underactuated states x and y . To regulate the fully actuated state z , a PD controller is designed by the difference between the current state z and the reference z_d as

$u_1 = -k_{vz}(\dot{z} - \dot{z}_d) - k_{pz}(z - z_d) + 1$, where k_{pz} and k_{vz} are positive real numbers that ensure z to converge to z_d . Then, one can have the closed-loop system for the altitude control $\ddot{z} = -k_{vz}(\dot{z} - \dot{z}_d) - k_{pz}(z - z_d)$. Since the desired altitude is constant, it is straightforward that $u_1 \equiv 1$ if the quadrotor keeps the given altitude z_d . By Eq. (2), the underactuated states x and y are driven by the current states θ and ϕ , respectively, which indicates that their references θ_d and ϕ_d can be treated as virtual control inputs. By letting v_x and v_y stand for the velocities in the x direction and the y direction, respectively, the virtual control inputs determined by the controllers for horizontal position control can be given by

$$\begin{aligned} \theta_d &= \frac{k_{vx}(v_x - v_{xd}) + k_{px}(x - x_d)}{u_1} \\ \phi_d &= \frac{k_{vy}(v_y - v_{yd}) + k_{py}(y - y_d)}{-u_1} \end{aligned} \quad (6)$$

where k_{vx} , k_{vy} , k_{px} , and k_{py} are positive real numbers that ensure the stability of the position control loop. It is worth mentioning that the initial error between z and z_d is commonly set to be small [19] to avoid the singularities.

By Eq. (6), the position (x, y) of the quadrotor in the horizontal xy plane can be adjusted by attitude controllers u_2 and u_3 since they can drive the states θ and ϕ to converge to the virtual control inputs θ_d and ϕ_d , respectively. By combining Eq. (6) with Eq. (2), and assuming that the inner-loop states are adjusted rapidly such that $\theta = \theta_d$ and $\phi = \phi_d$, one has

$$\begin{aligned} \dot{x}_1 &= x_2 \\ \dot{x}_2 &= -k_{vx}(x_2 - x_{2d}) - k_{px}(x_1 - x_{1d}) \\ \dot{x}_3 &= x_4 \\ \dot{x}_4 &= -k_{vy}(x_4 - x_{4d}) - k_{py}(x_3 - x_{3d}) \end{aligned} \quad (7)$$

where $x_1 \triangleq x$, $x_2 \triangleq v_x$, $x_3 \triangleq y$, and $x_4 \triangleq v_y$ are the states of position tracking in the xy plane. Note that in both the x direction and the y direction, the control objectives are to regulate the position and the velocity to the references, i.e., $\dot{x}_{2d} = \dot{x}_{4d} = 0$. By defining $e \triangleq x - x_d \triangleq [x_1 - x_{1d}, x_2 - x_{2d}, x_3 - x_{3d}, x_4 - x_{4d}]^T$, the closed-loop tracking error system can be represented as $\dot{e} = A_m e$, where the coefficient matrix is

$$A_m = \begin{bmatrix} 0 & 1 & 0 & 0 \\ -k_{px} & -k_{vx} & 0 & 0 \\ 0 & 0 & 0 & 1 \\ 0 & 0 & -k_{py} & -k_{vy} \end{bmatrix} \quad (8)$$

Note that, when the target motion is unmeasurable, a predictor will be utilized to provide an estimated position and velocity (derivative of position) of the target. Then, the existence of the reference signal can be ensured, which is denoted by $\hat{x}_d \triangleq [\hat{x}_{1d}, \hat{x}_{2d}, \hat{x}_{3d}, \hat{x}_{4d}]^T$. To regulate the states to \hat{x}_d , PD controllers with the same structure as Eq. (6) are designed, where the controller gains are denoted by k'_{px} , k'_{py} , k'_{vx} , and

k'_{vy} , and the closed-loop coefficient matrix is denoted by A_u . Clearly, the virtual control inputs and the matrix A_u in the case of losing the target can be obtained by replacing k_{px} , k_{py} , k_{vx} , and k_{vy} with k'_{px} , k'_{py} , k'_{vx} , and k'_{vy} in Eqs. (6) and (8), respectively. Hence, the tracking error system can be described by $\dot{e} = A_u(x - \hat{x}_d) = A_u(x - \hat{x}_d - x_d + x_d) = A_u e + A_u \Omega$, where $\Omega \triangleq x_d - \hat{x}_d$ stands for the prediction error that is the difference between actual values and estimated values of velocity and position of the target.

C. Switched System Formulation

In the tracking task of the quadrotor with intermittent measurements, the closed-loop tracking system can be split into two subsystems according to whether the target motion is measurable or not. The switching between subsystems will happen when the measurability of the target motion changes; then the underlying system will run in the corresponding subsystem. The switching signal for describing such a switching behavior is denoted by σ , which is a piecewise constant and right-continuous function [20,22]. Then, the switched closed-loop tracking system can be described by

$$\dot{e} = \begin{cases} A_m e & \sigma = 0 \\ A_u e + A_u \Omega & \sigma = 1 \end{cases} \quad (9)$$

where $\sigma = 0$ and $\sigma = 1$ refer to the measurable subsystem and the unmeasurable subsystem, respectively. It is straightforward that the error of the tracking system is exponentially convergent when $\sigma = 0$, while it may increase due to the existence of the prediction error Ω in the case of $\sigma = 1$. As commonly assumed in the existing literature [16], there exists a maximum running time T_{max}^+ of unmeasurable subsystems since the target may get out of the FOV in the case of long-time predicted position tracking. Then, the maximum prediction error can be obtained by T_{max}^+ and the maximum velocity of the target such that the disturbance on system convergence is bounded.

Unlike the existing studies that ignore the possible fast switching of measurable subsystems, the proposed new switched systems scheme covers the situation that the measurements may last shortly by formulating one stage of switching. As illustrated in Fig. 3, a switching stage is divided into a τ -portion and a \mathbb{T} -portion, where the τ -portion covers the activated measurable subsystem (denoted by m in Fig. 3) with running time greater than τ , and the \mathbb{T} -portion covers other rapid switching measurable subsystems and unmeasurable subsystems (denoted by u in Fig. 3). Thus, the running time conditions, i.e., the characteristic of the switching signal, can be expressed as $T_1^- \geq \tau$, $T_i^- < \tau (i > 1)$, and $T_i^+ \leq T_{max}^+$, where T_i^- and T_i^+ denote the running time of the i th activated measurable subsystem and unmeasurable subsystem, respectively, and i is upper bounded by the maximum number of activated times N in one stage.

Note that the existence of unmeasurable subsystems may lead to the increase of the system energy, where the possible values of the Lyapunov function are covered by dashed areas in Fig. 3. To ensure the convergence of the underlying system, the increase of system energy in the \mathbb{T} -portion should be counteracted by its decrease in the τ -portion, i.e., $\Delta V > 0$ (see Sec. IV for more details). Compared to the existing studies that treat a pair of continuous measurable subsystem and unmeasurable subsystem as one switching stage, it is more feasible to find a controller for the underlying system using the formulated switching stage in this paper since the sufficiently large

energy decrease of the measurable subsystems with short running time is not required to offset the energy increase in the unmeasurable subsystems.

Remark 1: If there exists only one activated unmeasurable subsystem in the \mathbb{T} -portion, i.e., the situation that the measurements last shortly is not encountered, the running time conditions will be converted into $T_1^- \geq \tau$ and $T_1^+ \leq T_{max}^+$. Thus, the formulated switching signal covers the dwell time switching signal as a special case.

Remark 2: The vector Ω contains predicted position errors and velocity errors in both x direction and y direction, where their upper bounds increase over time t . The upper bounds of the predicted errors do not depend on the adopted predictors since they are determined by the duration of losing the measurements and the maximum velocity of the target, so that the theoretical results obtained based on the upper bounds of the predicted errors are applicable for any predictor.

IV. Control Synthesis

In this section, we will develop stability conditions for the underlying system, upon which a switched controller with energy-dependent gains will be designed for quadrotor position control to achieve advantageous tracking performance.

A. Stability Analysis

For brevity, let $V \triangleq (1/2)e^T e$ denote the Lyapunov candidate for the quadrotor tracking system, and let $\zeta_m < 0$ and $\zeta_u < 0$ stand for the maximum eigenvalues of the matrices A_m and A_u , respectively. The following result holds.

Theorem 1: Consider the switched tracking system (9) and let $\lambda_s > 0$ be a given constant. If $T_1^- \geq \tau$ and $T_i^+ \leq T_{max}^+$ hold, the system is globally uniformly ultimately bounded (GUUB) for any switching signal satisfying

$$\tau \geq \frac{1}{\zeta_m} \ln \left(1 - \frac{S_k}{\sqrt{V}} \right) - \frac{\zeta_u \mathbb{T}}{\zeta_m} \quad (10)$$

where \bar{V} is the ultimate bound of the Lyapunov function, $S_k \leq (\sqrt{2}\lambda_s/2\zeta_u)(e^{\zeta_u \mathbb{T}} - 1)$ denotes the upper bound of the increase of the Lyapunov function in one stage, and $\mathbb{T} = NT_{max}^+$ is the maximum period of the \mathbb{T} -portion.

Proof: The Lyapunov functions are denoted by V_m and V_u for measurable subsystems and unmeasurable subsystems, respectively. It is straightforward that measurable subsystems are exponentially stable since

$$\dot{V}_m = e^T \dot{e} = e^T A_m e \leq 2\zeta_m V_m \quad (11)$$

When the target motion is unmeasurable, one has $\dot{V}_u = e^T \dot{e} = e^T (A_u e + A_u \Omega) = e^T A_u e + e^T A_u \Omega$. Let $\bar{\Omega} \triangleq [\Delta x, \Delta v_x, \Delta y, \Delta v_y]^T$ denote the upper bound of the prediction error at the maximum running time T_{max}^+ of unmeasurable subsystems. Then, the maximum increase of system energy can be computed as follows:

$$\begin{aligned} e^T A_u \bar{\Omega} &= k'_{px}(x_2 - x_{2d})\Delta x + (x_1 - x_{1d})\Delta v_x + k'_{vx}(x_2 - x_{2d})\Delta v_x \\ &\quad + k'_{py}(x_4 - x_{4d})\Delta y + (x_3 - x_{3d})\Delta v_y + k'_{vy}(x_4 - x_{4d}) \\ &\quad \times \Delta v_y \leq \lambda_s \|e\| \end{aligned} \quad (12)$$

where $\lambda_s \triangleq \Delta v_x + k'_{px}\Delta x + k'_{vx}\Delta v_x + \Delta v_y + k'_{py}\Delta y + k'_{vy}\Delta v_y$ is the prediction error coefficient. From $V_u = (1/2)e^T e$, $\|e\|$ is upper bounded by $\sqrt{2V_u}$. Then, we have

$$\dot{V}_u \leq 2\zeta_u V_u + \lambda_s \sqrt{2V_u} \quad (13)$$

The solutions to Eqs. (11) and (13) can be expressed by

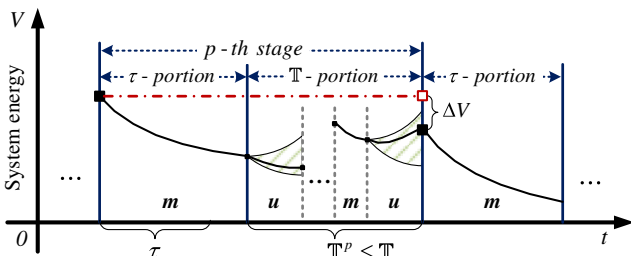


Fig. 3 Illustration of the scheme of the formulated switched system.

$$\begin{aligned} V_m(t) &\leq e^{2\zeta_m(t-t_0)} V_o(0) \\ V_u(t) &\leq \left(e^{\zeta_u(t-t_0)} \sqrt{V_u(0)} + \frac{\sqrt{2}\lambda_s}{2\zeta_u} (e^{\zeta_u(t-t_0)} - 1) \right)^2 \end{aligned} \quad (14)$$

For simplicity, the Lyapunov functions of the i th measurable subsystem and the i th unmeasurable subsystem are denoted as V_m^i and V_u^i in one stage, respectively. The value of the Lyapunov function at the end of the τ -portion satisfies

$$V_m^1(T_1^-) \leq e^{2\zeta_m T_1^-} V_m^1(0) \leq e^{2\zeta_m \tau} V_m^1(0) \quad (15)$$

Also, in the \mathbb{T} -portion, the final value of the Lyapunov function in one stage with $2N-1$ switches can be derived from the following inequalities:

$$\begin{aligned} V_u^N(T_N^+) &\leq \left(e^{\zeta_u T_N^+} \sqrt{V_u^N(0)} + \frac{\sqrt{2}\lambda_s}{2\zeta_u} (e^{\zeta_u T_N^+} - 1) \right)^2 \\ &\leq \left(e^{\zeta_u T_N^+ + \zeta_m T_N^-} \sqrt{V_m^N(0)} + \frac{\sqrt{2}\lambda_s}{2\zeta_u} (e^{\zeta_u T_N^+} - 1) \right)^2 \\ &\leq \left(e^{\zeta_u T_N^+ + \zeta_m T_N^- + \zeta_u T_{N-1}^+} \sqrt{V_u^{N-1}(0)} \right. \\ &\quad \left. + e^{\zeta_u T_N^+ + \zeta_m T_N^-} \frac{\sqrt{2}\lambda_s}{2\zeta_u} (e^{\zeta_u T_{N-1}^+} - 1) + \frac{\sqrt{2}\lambda_s}{2\zeta_u} (e^{\zeta_u T_N^+} - 1) \right)^2 \\ &\quad \vdots \\ &\leq \left(e^{\zeta_u \sum_{i=1}^N T_i^+ + \zeta_m \sum_{i=2}^N T_i^-} \sqrt{V_u^1(0)} \right. \\ &\quad \left. + \frac{\sqrt{2}\lambda_s}{2\zeta_u} \sum_{i=1}^N (e^{\zeta_u T_{N-i+1}^+} - 1) e^{\sum_{k=1}^i (\zeta_u T_k^+ + \zeta_m T_k^-)} \right)^2 \\ &= (e^{\zeta_u \sum_{i=1}^N T_i^+ + \zeta_m \sum_{i=2}^N T_i^-} \sqrt{V_u^1(0)} + S_k)^2 \end{aligned} \quad (16)$$

By combining Eqs. (15) and (16), and considering the worst cases $T_i^- \equiv 0$ and $T_i^+ \equiv T_{\max}^+$ in the \mathbb{T} -portion, it can be derived that

$$\begin{aligned} V_u^N(T_N^+) &\leq (e^{\zeta_u \sum_{i=1}^N T_i^+ + \zeta_m \sum_{i=2}^N T_i^- + \zeta_m T_1^-} \sqrt{V_m^1(0)} + S_k)^2 \\ &\leq (e^{\zeta_u N T_{\max}^+ + \zeta_m (N-1) T_{\min}^- + \zeta_m T_1^-} \sqrt{V_m^1(0)} + S_k)^2 \\ &\leq (e^{\zeta_u \mathbb{T} + \zeta_m \tau} \sqrt{V_m^1(0)} + S_k)^2 \end{aligned} \quad (17)$$

where S_k satisfies

$$\begin{aligned} S_k &\leq \frac{\sqrt{2}\lambda_s}{2\zeta_u} \sum_{i=1}^N (e^{\zeta_u T_{\max}^+} - 1) e^{\sum_{k=1}^i (\zeta_u T_{\max}^+ + \zeta_m T_{\min}^-)} \\ &\leq \frac{\sqrt{2}\lambda_s}{2\zeta_u} (e^{\zeta_u T_{\max}^+} - 1) \sum_{i=1}^N e^{(N-i)(\zeta_u T_{\max}^+ + \zeta_m T_{\min}^-)} \\ &\leq \frac{\sqrt{2}\lambda_s}{2\zeta_u} (e^{\zeta_u T_{\max}^+} - 1) \frac{1 - e^{N(\zeta_u T_{\max}^+ + \zeta_m T_{\min}^-)}}{1 - e^{\zeta_u T_{\max}^+ + \zeta_m T_{\min}^-}} \\ &\leq \frac{\sqrt{2}\lambda_s}{2\zeta_u} (e^{\zeta_u \mathbb{T}} - 1) \end{aligned} \quad (18)$$

To ensure the stability of the tracking system, the initial value of the Lyapunov function should decrease between consecutive stages. By letting the upper bound of the final value of the Lyapunov function $(e^{\zeta_u \mathbb{T} + \zeta_m \tau} \sqrt{V_m^1(0)} + S_k)^2$ be no larger than the initial value $V_m^1(0)$ in each stage, we have

$$\sqrt{V_m^1(0)} \geq \frac{S_k}{1 - e^{\zeta_u \mathbb{T} + \zeta_m \tau}} \quad (19)$$

which means that the initial value of each stage decreases until it is equal to the final value, i.e., $V_u^N(T_N^+) = (e^{\zeta_u \mathbb{T} + \zeta_m \tau} \sqrt{V_m^1(0)} + S_k)^2 = V_m^1(0)$. Since the value of the Lyapunov function is always not greater than the initial value $V_m^1(0)$, the system energy will be bounded by

$$V(t) \leq \left(\frac{S_k}{1 - e^{\zeta_u \mathbb{T} + \zeta_m \tau}} \right)^2 \leq \bar{V}, \quad t \rightarrow \infty \quad (20)$$

which is equivalent to Eq. (10). Thus, the proof is completed. \square

Remark 3: The target tracking task with intermittent measurements can be modeled by a dwell time switched system [16], which is a special case of the switched system formulated in this paper. By letting $N = 1$ in Eq. (17), the GUUB condition for the dwell time switched system can be obtained as

$$\tau \geq \frac{1}{\zeta_m} \ln(1 - \lambda_s (e^{\zeta_u T} - 1) / (\zeta_u \sqrt{2\bar{V}})) - \frac{\zeta_u T}{\zeta_m}$$

where T is the maximum running time of unmeasurable subsystems.

B. Switched Control Design

It can be seen from Eq. (10) that there exists a connection among the ultimate bound of the system energy, the running time of subsystems, and the controller gains. In the existing literature [15–17], the running time conditions are determined by the predesigned controllers for subsystems, which applies only to the stability analysis for the underlying system. In this paper, the controller design for the whole switched system will be investigated, which is more applicable and significant but has not been considered in target tracking of quadrotors with intermittent measurements.

The steady-state performance of the switched system of target tracking with intermittent measurements can be improved by reducing the ultimate bound on the system energy. By combining Eqs. (18) and (20), one has

$$V(t) = \left(\frac{\sqrt{2}\lambda_s}{2\zeta_u} \frac{(1 - e^{\zeta_u \mathbb{T}})}{(1 - e^{\zeta_u \mathbb{T} + \zeta_m \tau})} \right)^2 < \left(\frac{\sqrt{2}\lambda_s}{2\zeta_u} \right)^2 \quad (21)$$

It is worth noting that since the number of switching times N is unknown a priori in practice, the worst case that the measurable subsystem with running time greater than τ cannot be activated is considered in Eq. (21), i.e., $N \rightarrow \infty$, $\mathbb{T} \rightarrow \infty$. The maximum eigenvalue of A_u in Eq. (9) can be computed by $\zeta_u = -(1/2) \min\{k'_{vx} \pm \sqrt{k_{vx}^2 - 4k'_{px}}, k'_{vy} \pm \sqrt{k_{vy}^2 - 4k'_{py}}\}$. By defining the proportional coefficients $\gamma_x \triangleq (k'_{vx}/k'_{px})$ and $\gamma_y \triangleq (k'_{vy}/k'_{py})$, and taking $\zeta_u = (1/2)(-k'_{vx} + \sqrt{k_{vx}^2 - 4k'_{px}})$ as an example, the square root of the ultimate bound can be given by

$$\begin{aligned} \left| \frac{\sqrt{2}\lambda_s}{2\zeta_u} \right| &= \sqrt{2} \cdot \frac{k'_{px} \Delta x + (1 + k'_{vx}) \Delta v_x + k'_{py} \Delta y + (1 + k'_{vy}) \Delta v_y}{k'_{vx} - \sqrt{k_{vx}^2 - 4k'_{px}}} \\ &= \sqrt{2} \left(\frac{k'_{px} \Delta x + \gamma_x k'_{px} \Delta v_x}{\gamma_x k'_{px} - \sqrt{\gamma_x^2 k_{px}^2 - 4k'_{px}}} + \frac{\Delta v_x + k'_{py} \Delta y + (1 + \gamma_y k'_{py}) \Delta v_y}{\gamma_x k'_{px} - \sqrt{\gamma_x^2 k_{px}^2 - 4k'_{px}}} \right) \end{aligned} \quad (22)$$

It is straightforward that the ultimate bound of the system energy can be reduced by decreasing the value of k'_{px} or γ_x . The analysis for the connection between the ultimate bound and the value of k'_{py} or γ_y is similar to the one for k'_{px} or γ_x , respectively; then the ultimate bound increases if the value of k'_{py} or γ_y rises. Thus, the ultimate bound of the Lyapunov function of the underlying system can be reduced by decreasing the controllers gains (k'_{px} , k'_{py} , k'_{vx} , k'_{vy}) in the case of losing the target.

Considering quadrotor dynamics (2) and the horizontal position controllers (6), it can be observed that the controller gains in A_u are proportional to the accelerations of the quadrotor, which should not decrease immoderately since small accelerations may cause that the target gets out of the FOV of the on-board sensors or the approaching time is lengthened.

To ensure the rapid approaching capability of the quadrotor, the tracking system must converge fast. Let μ denote the convergence coefficient of one stage, which can be computed by

$$\begin{aligned} \mu &= \frac{V_u^N(T_N^+)}{V_m^1(0)} = \left(e^{\zeta_1 T + \zeta_2 \tau} + \frac{\sqrt{2}\lambda}{2\zeta_u \sqrt{V_m^1(0)}} (e^{\zeta_u T} - 1) \right)^2 \\ &\leq \left(e^{\zeta_u T + \zeta_m \tau} + \frac{\sqrt{2}\lambda_s}{2\zeta_u \sqrt{V_m^1(0)}} (e^{\zeta_u T} - 1) \right)^2 \end{aligned} \quad (23)$$

where λ is determined by actual prediction errors satisfying $\lambda \leq \lambda_s$, and ζ_1 and ζ_2 are the actual convergence rates of the measurable subsystem states and the unmeasurable subsystem states under the initial value at the current stage, respectively. In the target tracking process, it is often encountered that the target is far away from the quadrotor ($(x - x_d/v_x - v_{xd}) \gg \gamma_x$ or $(y - y_d/v_y - v_{yd}) \gg \gamma_y$), and the prediction error is small ($\sqrt{V_m^1(0)} \gg \lambda$). Under such circumstances, the convergence coefficient μ will decrease if the controller gains increase, which means that the gains with large values in A_u enable the system energy to decrease rapidly.

Considering the transient-state performance and steady-state performance of the underlying system simultaneously, an energy-dependent switched controller \mathbb{U}^* is designed, where the gains in A_m are constant and the gains in A_u are determined by

$$\frac{\sqrt{V_m^1(0)}}{2} = \frac{1}{\sqrt{\mu}} \cdot \frac{k'_{px} \Delta x + (1 + k'_{vx}) \Delta v_x + k'_{py} \Delta y + (1 + k'_{vy}) \Delta v_y}{\min\{k'_{vx} \pm \sqrt{k'_{vx}{}^2 - 4k'_{px}}, k'_{vy} \pm \sqrt{k'_{vy}{}^2 - 4k'_{py}}\}} \quad (24)$$

in each stage. It is worth noting that the utilized gains in A_u should be upper bounded by the ones in A_m in the tracking process since the gains in A_m have been set as large as possible for ensuring the rapid response capability of the quadrotor when the target can be measured. By setting $\mu < 1$, the upper bound of system energy in the current stage will be less than the initial energy, which ensures the convergence of the tracking system.

Figure 4a shows the workflow of the quadrotor tracking control by applying the designed switched controller with energy-dependent gains. The initial time in each stage should be determined according to whether the running time of the measurable subsystem is greater than τ ; next the controller gains in A_u are solved by Eq. (24). It is worth mentioning that if $\mathbb{T}^{(p)} > \mathbb{T}$ holds, i.e., the target cannot be measured for a long time, the quadrotor will hover and wait for a new command. The variations of the controller gains and the system energy are shown

in Fig. 4b, where the gains in A_u decrease as the stage increases since the initial value $V_m^1(0)$ of the Lyapunov function of each stage decreases. Then, the ultimate bound of system energy will decrease, which indicates that the tracking error will be as small as possible.

Remark 4: The designed switched controller with energy-dependent gains provides large accelerations for target tracking with the stability guarantee in each stage. By using the controller, the quadrotor will approach the target rapidly when the quadrotor is far away from the target or the predicted position is fairly accurate, while in the case that the predicted position is completely wrong, i.e., the prediction error reaches its upper bound, the convergence of system energy can still be guaranteed.

Remark 5: Compared to the traditional switched controller, the designed switched controller with energy-dependent gains has the advantage of alleviating the control bump [23] that is defined by the difference between the values of control inputs before and after subsystems switching. From Fig. 4, the difference in gains at the switching instants gradually increases as the tracking error decreases, which avoids a dramatic control bump since the control inputs are determined by the product of gains and tracking error. This is in contrast with the traditional switched controller, where dramatic control bumps may occur in the cases of large tracking error caused by using constant gains in each subsystem.

V. Simulations

In this section, three general scenarios of quadrotor tracking control with intermittent measurements of a certain target are provided to demonstrate the effectiveness of the obtained theoretical results and the superiority of the switched control design.

To show the feasibility of the switched control design under the energy-dependent gains, we shall first check the relation between the ultimate bound of the system energy and the controller gains ($k'_{px}, k'_{py}, k'_{vx}, k'_{vy}$) when the target cannot be measured, as shown in Theorem 1. Here, two different trajectories of the target are considered, which is tracked by the quadrotor using the controllers with various gains.

The first trajectory of the target is governed by the static equations $x_t = 0.25t + 21$ and $y_t = 0.625t + 21$, which implies that the target moves along a straight line with constant velocity. The initial position of the quadrotor is set as $(0, 0)$ in xy plane at the tracking frame \mathcal{F}_t , and the reference signals are assigned as $x_d = x_t$ and $y_d = y_t$ when the target can be measured. Once the measurements are unavailable, a zero-order holder is utilized to predict the position of the target [24], which assumes that the target stays at the position of the instant that the measurements are lost. The switching signals to describe the phenomenon of intermittent measurements satisfy $\tau = 3$, $T_i^- = 1$ ($i > 1$), $T_i^+ = 6$, and $\mathbb{T} = 27$, where the considered durations of subsystems are the same in each stage. In the tracking process, the reference signal of the heading angle is set to be constant and assigned as $\psi_d = 0$, and the desired values θ_d and ϕ_d are obtained from Eq. (6), where the initial attitude angles of the quadrotor are $\theta(0) = \phi(0) = \psi(0) = 0$. To regulate the quadrotor attitude, the NNTSMC-based controllers of the form as Eq. (4) with $\beta = 0.2$, $p = 5$, $q = 3$,

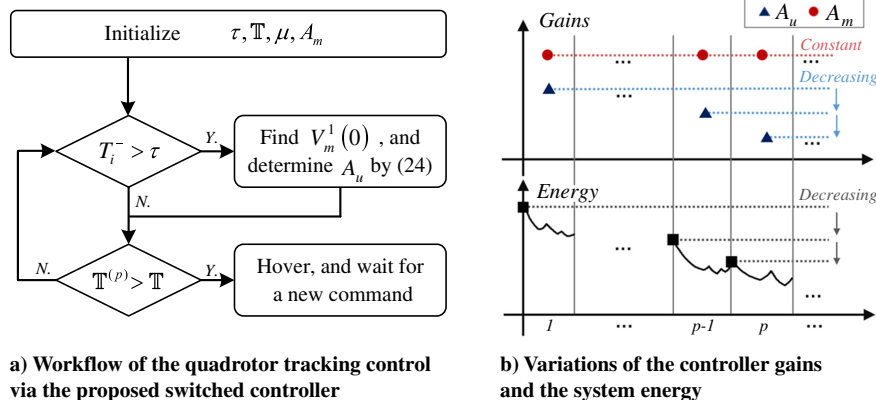


Fig. 4 Illustration of the designed switched controller with energy-dependent gains.

and $K = 5$ are utilized. It is worth mentioning that the adopted quadrotor dynamics is the nonlinear model (1) instead of the linearized one in all simulations; so the accuracy of linearization can be demonstrated simultaneously since the utilized controllers are derived by the linearized model (2) of the quadrotor.

To illustrate the influence of using different controller gains on the tracking performance, 10 controllers are adopted for tracking an intermittently measured target. Figure 5a shows the energy variations of the tracking system and the quadrotor trajectories under the utilization of different controllers, where the controller gains when the target is measurable are identical and they are set to be $k_{px} = k_{py} = 0.01$ and $k_{vx} = k_{vy} = 0.3$. In the case of losing the target, the gains of 10 different controllers are set as $k'_{vx} = k'_{vy} = 30k'_{px} = 30k'_{py}$, where k'_{px} are 10 points selected in the interval $[0.005, 0.025]$. It can be observed that decreasing the controller gains helps reduce the increment of system energy when the target cannot be measured; as a result, the ultimate bound of the Lyapunov function also decreases. The influence of the proportional coefficient $\gamma_x(\gamma_y)$ on tracking performance is shown in Fig. 5b. The controller gains are set to be $30k_{px} = 30k_{py} = k_{vx} = k_{vy} = 0.3$ and $k'_{vx} = k'_{vy} = \gamma_x k'_{px} = \gamma_y k'_{py} = 0.01\gamma_x$, where $\gamma_x = \gamma_y \in [25, 50]$. One can observe that the ultimate bound of the Lyapunov function can be reduced by decreasing the proportional coefficient $\gamma_x(\gamma_y)$, while using small $\gamma_x(\gamma_y)$ will result in oscillations of the system energy. Hence, the effectiveness of the connection between the controller gains and the ultimate bound of system energy obtained by Theorem 1 is verified.

The second trajectory of the target is set in accordance with the equations $x_t = 1 + 5 \cos 0.0125\pi t$ and $y_t = 1 + 5 \sin 0.0125\pi t$, which implies that the target moves along a circle with time-varying velocities in both x and y directions. The predictor, the switching signal, the initial states of the quadrotor, and the attitude controllers are set to be the same as the ones adopted in tracking the target with the first trajectory. The controller gains when the target can be measured are set to be $k_{px} = k_{py} = 0.1$ and $k_{vx} = k_{vy} = 1$. Figure 5c shows the tracking performance by using different controller gains

when the measurements are unavailable, where $k'_{px} \in [0.04, 0.20]$ and other gains are determined by $k'_{vx} = k'_{vy} = 10k'_{px} = 10k'_{py}$. In Fig. 5d, various proportional coefficients γ_x are utilized in the case of losing the target, where $\gamma_x \in [7, 25]$ and other controller gains are set as $k'_{vx} = k'_{vy} = \gamma_x k'_{px} = \gamma_y k'_{py} = 0.1\gamma_x$. It can be readily verified that the reduction of the controller gains $k'_{px}(k'_{py})$ or proportional coefficients $\gamma_x(\gamma_y)$ can decrease the ultimate bound of the system energy such that the performance of target tracking is improved, which shows the effectiveness of the relation built by Theorem 1 in tracking a target with time-varying velocities.

In Fig. 5, the red-star lines stand for the cases of no controller switching, where the selected gains in A_u are the same as the ones in A_m . The blue triangles stand for the final positions of the target with different trajectories, while other triangles are the quadrotor final positions by using the controllers with different gains. It can be seen that switching to a controller with smaller gains in the case of losing the target will achieve lower system energy and fewer tracking errors in the steady state compared with nonswitching controllers, which indicates that the controller switching is necessary and beneficial in the target tracking task with intermittent measurements.

Now, we turn to the demonstration of the superiority of the proposed switched control design. In the previous scenarios, the controllers were predesigned, and they could not obtain desired transient and steady-state performance simultaneously. To show the performance of the designed switched controller with energy-dependent gains, the whole process of quadrotor control for target tracking with intermittent measurements is considered. Also, a more general trajectory of the target is set as follows:

$$x_t = \begin{cases} 25 + 0.15625t - 2 \cos 0.025\pi t, & 0 \leq t < 64 \\ 45 - 0.15625t - 2 \cos 0.025\pi t, & 64 \leq t \leq 150 \end{cases}$$

$$y_t = \begin{cases} 30 + 0.15625t + 2 \sin 0.025\pi t, & 0 \leq t < 24 \\ 37.5 - 0.15625t + 2 \sin 0.025\pi t, & 24 \leq t \leq 150 \end{cases}$$

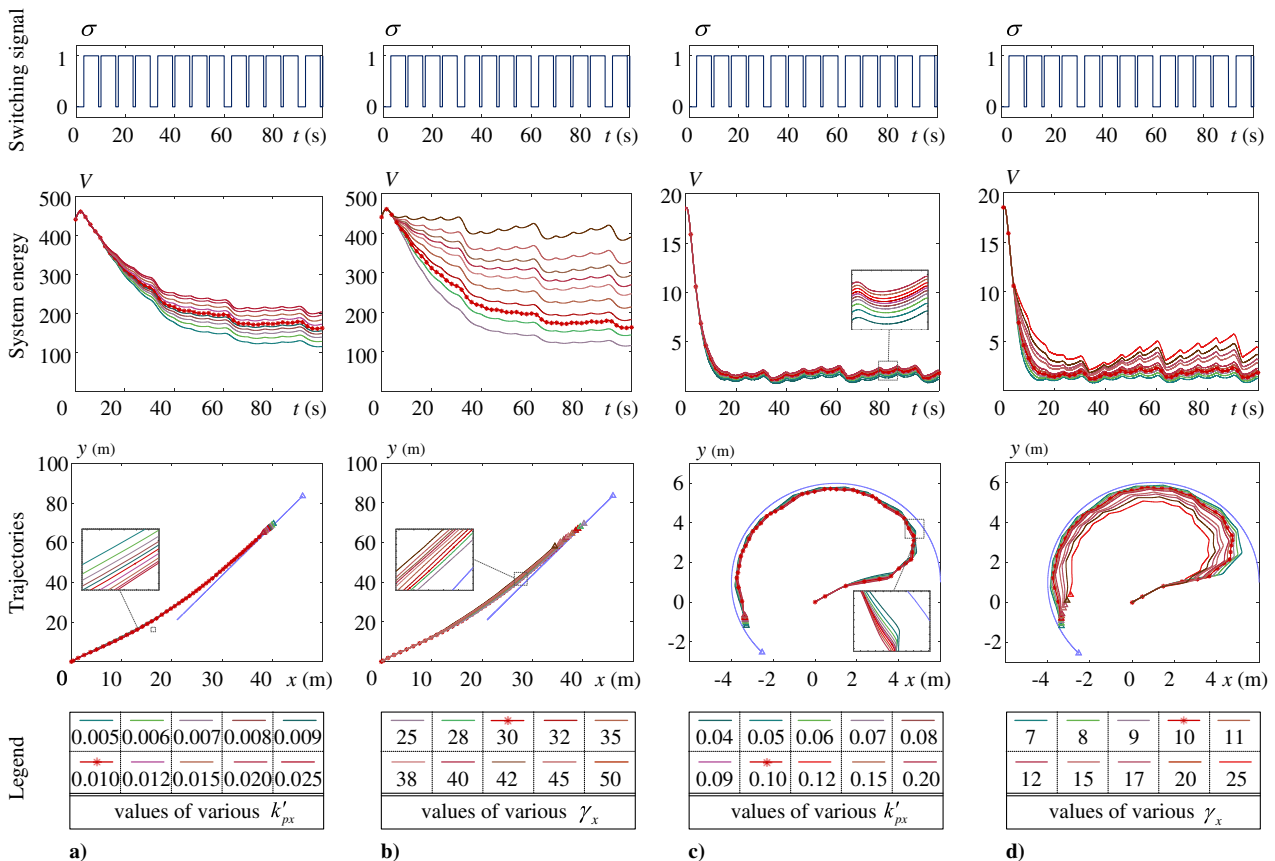


Fig. 5 Tracking performance under the proposed switched systems scheme with different controller gains.

The quadrotor is desired to track the target by the references $x_d = x_t$, $y_d = y_t$, $z_d = 4$, and $\psi_d = 0$, where the initial values of quadrotor states are set as $[x(0) \ y(0) \ z(0) \ \theta(0) \ \phi(0) \ \psi(0)]^T = [0 \ 0 \ 0 \ 0 \ 0 \ 0]^T$. The switching signal is generated randomly under the running time conditions $\tau = 3$ and $T_{\max}^+ = 4$ such that both fast switching and slow switching phenomena can be covered. Once the target is lost, a predictor that assumes that the target moves with the same velocity at the instant that the measurements are lost is utilized. When the quadrotor is close to the target, the measurements are assumed not to be lost.

To verify the advantages of the designed switched controller with energy-dependent gains, we take another two predesigned controllers with different gains for comparison. When the target can be measured, the gains of the adopted controllers are set to be the same, where $k_{px} = k_{py} = 0.015$ and $k_{vx} = k_{vy} = 0.45$. When the target cannot be measured, the gains of the controllers are set as follows:

- i) Let \mathbb{U}_1 denote the nonswitched controller, where $k'_{px} = k'_{py} = k_{px}$ and $k'_{vx} = k'_{vy} = k_{vx}$.
- ii) The second controller is denoted by \mathbb{U}_2 , where the gains are predesigned and they are set to be $k'_{px} = k'_{py} = k'_{vx} = k'_{vy} = 0$.
- iii) \mathbb{U}^* stands for the designed switched controller with energy-dependent gains, where the gains are determined by the workflow in Fig. 4 with the selected convergence coefficient $\mu = 0.4$.

The obtained gains in first stage and second stage are $k'_{px} = 0.012$ and $k'_{py} = 0.0065$, respectively, and other parameters are determined by $k'_{px} = k'_{py} = (1/30)k_{vx} = (1/30)k_{vy}$. In other stages, the gains are set to be the smallest ones $k'_{px} = k'_{py} = k'_{vx} = k'_{vy} = 0$ since

there is no solution to Eq. (24); i.e., the underlying system has reached the steady state and its initial energy value of the current stage has been fairly small.

Based on the adopted controllers, the variations of the Lyapunov function of the closed-loop tracking system under the same initial conditions are shown in Fig. 6. The proposed switched controller with energy-dependent gains \mathbb{U}^* achieves better performance than the nonswitched controller \mathbb{U}_1 and the predesigned switched controller \mathbb{U}_2 . Compared with \mathbb{U}_1 , the controllers \mathbb{U}^* and \mathbb{U}_2 with lower gains show their capability of overcoming the energy increase caused by the prediction error and reducing the upper bound of the Lyapunov function. Also, \mathbb{U}^* outperforms \mathbb{U}_2 in terms of transient-state performance in the approaching process or when the prediction position does not deviate much from the actual position. In addition, using controller \mathbb{U}^* , the quadrotor approaches the target rapidly and keeps the tracking errors as small as possible, where the variations of piecewise continuous virtual control inputs θ_d and ϕ_d for quadrotor horizontal position control are shown in Fig. 7a; while actual positions (red parts) and estimated positions (gray parts) of the target and the trajectory of the quadrotor are shown in Fig. 7b, where z axis is the difference with respect to the initial value. Unlike the predesigned controllers that focus on reducing steady-state errors and ignore the transient-state performance, the designed switched controller with energy-dependent gains drives the quadrotor by various gains in different stages in the case of losing the target, which ensures both transient-state performance and steady-state performance. Hence, the designed switched controller with energy-dependent gains outperforms the nonswitched controller and the predesigned switched controller, which demonstrates the superiority of the switched control design.

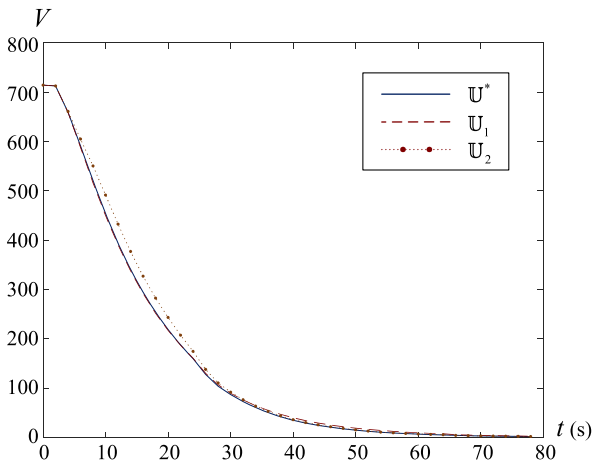
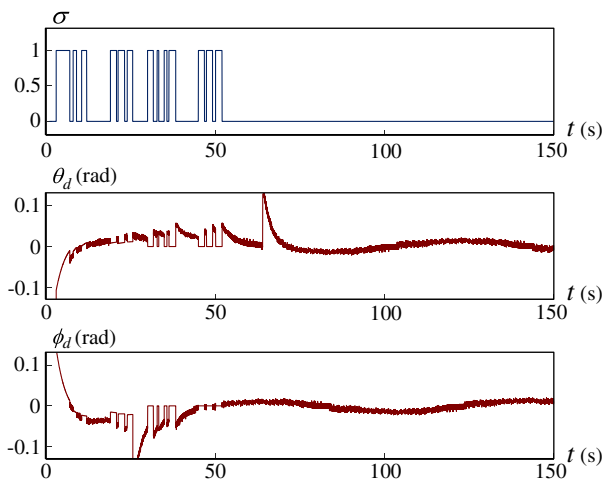


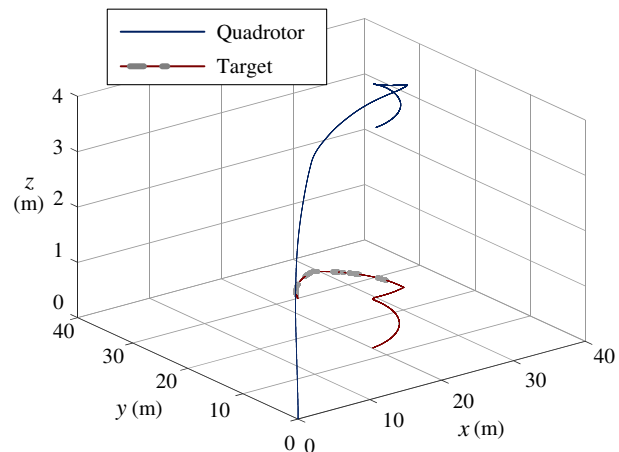
Fig. 6 Variations of the Lyapunov function by adopting different controllers.

VI. Conclusions

The problem of target tracking control of the quadrotor with complex intermittent measurements was investigated in this paper. A new switched systems scheme was formulated to cover the case when measurements last shortly, which was not considered before. Different from the existing studies that focus on the stability analysis for the underlying system based on predesigned controllers, a switched controller with energy-dependent gains was designed such that the quadrotor approaches the target rapidly and keeps a small tracking error as much as possible. Simulation results show the superiority of the designed switched controller in the tracking task of the quadrotor, where the feedback is temporarily available. In the future, it is expected to employ the designed switched controller on a real quadrotor together with the corresponding target detection method to accomplish the target tracking tasks with intermittent measurements in practice, and the proposed formulation and switched control methods can be extended to other target tracking



a) Virtual control inputs



b) Trajectories of target and quadrotor

Fig. 7 Illustration of tracking control of the quadrotor using designed switched controller \mathbb{U}^* .

tasks with intermittent measurements of other unmanned systems, such as unmanned ground vehicles, and robotic arms.

Acknowledgments

This work was supported in part by National Natural Science Foundation of China under Grant 62225305, Grant 12072088, Grant 62003117, and Grant 62003118; in part by the Grant JCKY2020603B010; and in part by Natural Science Foundation of Heilongjiang Province, China, under Grant ZD2020F001.

References

- [1] Yang, H. C., AbouSleiman, R., Sababha, B., Gjioni, E., Korff, D., and Rawashdeh, O., "Implementation of an Autonomous Surveillance Quadrotor System," *AIAA Infotech Aerospace Conference*, AIAA Paper 2009-2047, 2009.
<https://doi.org/10.2514/6.2009-2047>
- [2] Bhandari, S., Viska, S., Shah, H., Chen, C., Tonini, G., and Kline, S., "Autonomous Navigation of a Quadrotor in Indoor Environments for Surveillance and Reconnaissance," *AIAA Infotech Aerospace Conference*, AIAA Paper 2015-0717, 2015.
<https://doi.org/10.2514/6.2015-0717>
- [3] Kaya, D., Kutay, A. T., Kurtulus, D. F., Tekinalp, O., Simsek, I., Soysal, S., and Hosgit, G., "Propulsion System Selection and Modeling for a Quadrotor with Search and Rescue Mission," *54th AIAA Aerospace Sciences Meeting*, AIAA Paper 2016-1528, 2016.
<https://doi.org/10.2514/6.2016-1528>
- [4] Borowczyk, A., Nguyen, D.-T., Nguyen, A. P.-V., Nguyen, D. Q., Saussié, D., and Le Ny, J., "Autonomous Landing of a Quadcopter on a High-Speed Ground Vehicle," *Journal of Guidance, Control, and Dynamics*, Vol. 40, No. 9, 2017, pp. 2378–2385.
<https://doi.org/10.2514/1.G002703>
- [5] Lu, Q., Ren, B., and Parameswaran, S., "Shipboard Landing Control Enabled by an Uncertainty and Disturbance Estimator," *Journal of Guidance, Control, and Dynamics*, Vol. 41, No. 7, 2018, pp. 1502–1520.
<https://doi.org/10.2514/1.G003073>
- [6] Ai, X., and Yu, J., "Fixed-Time Trajectory Tracking for a Quadrotor with External Disturbances: A Flatness-Based Sliding Mode Control Approach," *Aerospace Science and Technology*, Vol. 89, Dec. 2019, pp. 58–76.
<https://doi.org/10.1016/j.ast.2019.03.059>
- [7] Maurya, H. L., Kamath, A. K., Verma, N. K., and Behera, L., "Vision-Based Fractional Order Sliding Mode Control for Autonomous Vehicle Tracking by a Quadrotor UAV," *2019 28th IEEE International Conference on Robot and Human Interactive Communication (RO-MAN)*, Inst. of Electrical and Electronics Engineers, New York, 2019, pp. 1–6.
<https://doi.org/10.1109/RO-MAN46459.2019.8956317>
- [8] Shao, X., Liu, N., Wang, Z., Zhang, W., and Yang, W., "Neuroadaptive Integral Robust Control of Visual Quadrotor for Tracking a Moving Object," *Mechanical Systems and Signal Processing*, Vol. 136, May 2020, Paper 106513.
<https://doi.org/10.1016/j.ymssp.2019.106513>
- [9] Zhao, W., Liu, H., Lewis, F. L., Valavanis, K. P., and Wang, X., "Robust Visual Servoing Control for Ground Target Tracking of Quadrotors," *IEEE Transactions on Control Systems Technology*, Vol. 28, No. 5, 2019, pp. 1980–1987.
<https://doi.org/10.1109/TCST.2019.2922159>
- [10] Ristevski, S., Koru, A. T., Yucelen, T., Dogan, K. M., and Muse, J. A., "Experimental Results of a Quadrotor UAV with a Model Reference Adaptive Controller in the Presence of Unmodeled Dynamic," *AIAA Scitech 2022 Forum*, AIAA Paper 2022-1381, 2022.
<https://doi.org/10.2514/6.2022-1381>
- [11] Shastry, A. K., Sinha, H., and Kothari, M., "Autonomous Detection and Tracking of a High-Speed Ground Vehicle Using a Quadrotor UAV," *AIAA Scitech 2019 Forum*, AIAA Paper 2019-1188, 2019.
<https://doi.org/10.2514/6.2019-1188>
- [12] Parikh, A., Kamalapurkar, R., and Dixon, W. E., "Target Tracking in the Presence of Intermittent Measurements via Motion Model Learning," *IEEE Transactions on Robotics*, Vol. 34, No. 3, 2018, pp. 805–819.
<https://doi.org/10.1109/TRO.2018.2821169>
- [13] Zhang, J., You, K., and Xie, L., "Bayesian Filtering with Unknown Sensor Measurement Losses," *IEEE Transactions on Control of Network Systems*, Vol. 6, No. 1, 2018, pp. 163–175.
<https://doi.org/10.1109/TCNS.2018.2802872>
- [14] Penin, B., Giordano, P. R., and Chaumette, F., "Vision-based Reactive Planning for Aggressive Target Tracking While Avoiding Collisions and Occlusions," *IEEE Robotics and Automation Letters*, Vol. 3, No. 4, 2018, pp. 3725–3732.
<https://doi.org/10.1109/LRA.2018.2856526>
- [15] Chen, H.-Y., Bell, Z., Licitra, R., and Dixon, W., "A Switched Systems Approach to Vision-Based Tracking Control of Wheeled Mobile Robots," *2017 IEEE 56th Annual Conference on Decision and Control*, Inst. of Electrical and Electronics Engineers, New York, 2017, pp. 4902–4907.
<https://doi.org/10.1109/CDC.2017.8264384>
- [16] Zhang, L., Wang, S., Cai, B., Liu, T., and Cheng, Y., "Switching Control of a Mecanum Wheeled Mobile Robot for Vision-Based Tracking with Intermittent Image Losses," *2019 IEEE International Conference on Systems, Man and Cybernetics (SMC)*, Inst. of Electrical and Electronics Engineers, New York, 2019, pp. 493–499.
<https://doi.org/10.1109/SMC.2019.8914160>
- [17] Carrillo, L. R. G., Colunga, G. R. F., Sanahuja, G., and Lozano, R., "Quad Rotorcraft Switching Control: An Application for the Task of Path Following," *IEEE Transactions on Control Systems Technology*, Vol. 22, No. 4, 2013, pp. 1255–1267.
<https://doi.org/10.1109/TCST.2013.2284790>
- [18] Lanzon, A., Freddi, A., and Longhi, S., "Flight Control of a Quadrotor Vehicle Subsequent to a Rotor Failure," *Journal of Guidance, Control, and Dynamics*, Vol. 37, No. 2, 2014, pp. 580–591.
<https://doi.org/10.2514/1.59869>
- [19] Gomez-Balderas, J.-E., Flores, G., Carrillo, L. G., and Lozano, R., "Tracking a Ground Moving Target with a Quadrotor Using Switching Control," *Journal of Intelligent & Robotic Systems*, Vol. 70, No. 1, 2013, pp. 65–78.
<https://doi.org/10.1007/s10846-012-9747-9>
- [20] Hespanha, J. P., "Uniform Stability of Switched Linear Systems: Extensions of LaSalle's Invariance Principle," *IEEE Transactions on Automatic Control*, Vol. 49, No. 4, 2004, pp. 470–482.
<https://doi.org/10.1109/TAC.2004.825641>
- [21] Feng, Y., Yu, X., and Man, Z., "Non-Singular Terminal Sliding Mode Control of Rigid Manipulators," *Automatica*, Vol. 38, No. 12, 2002, pp. 2159–2167.
[https://doi.org/10.1016/S0005-1098\(02\)00147-4](https://doi.org/10.1016/S0005-1098(02)00147-4)
- [22] Zhang, L., Zhu, Y., Shi, P., and Lu, Q., *Time-Dependent Switched Discrete-Time Linear Systems: Control and Filtering*, Springer, Berlin, 2016, Chap. 1.
<https://doi.org/10.1007/978-3-319-28850-5>
- [23] Zhang, L., Xu, K., Yang, J., Han, M., and Yuan, S., "Transition-Dependent Bumpless Transfer Control Synthesis of Switched Linear Systems," *IEEE Transactions on Automatic Control*, Vol. 2022, Feb. 2022, pp. 1–11.
<https://doi.org/10.1109/TAC.2022.3152721>
- [24] Parikh, A., Cheng, T.-H., Licitra, R., and Dixon, W., "A Switched Systems Approach to Image-Based Localization of Targets that Temporarily Leave the Camera Field of View," *IEEE Transactions on Control Systems Technology*, Vol. 26, No. 6, 2017, pp. 2149–2156.
<https://doi.org/10.1109/TCST.2017.2753163>